ACCELERATED DOCUMENT DISTRIBUTION SYSTEM

REGULATORY INFORMATION DISTRIBUTION SYSTEM (RIDS)

ACCESSION NBR:9305240056 DOC.DATE: 93/05/14 NOTARIZED: NO DOCKET #
FACIL:50-410 Nine Mile Point Nuclear Station, Unit 2, Niagara Moha 05000410
AUTH.NAME AUTHOR AFFILIATION
TERRY,C.D. Niagara Mohawk Power Corp.
RECIP.NAME RECIPIENT AFFILIATION
Document Control Branch (Document Control Desk)

SUBJECT: Forwards paper entitled, "Improved Influence Functions for Part-Circumferential Cracks in Pipes," per 930428 telcon re util 930316 submittal of results of most recent fracture mechanics analysis on weld KC-32.

DISTRIBUTION CODE: A001D COPIES RECEIVED:LTR 1 ENCL 1 SIZE: 15
TITLE: OR Submittal: General Distribution

NOTES:

	RECIPIENT ID CODE/NAME		COPIES LTTR	COPIES ENCL	RECIPIENT ID CODE/NAME	COPIES LTTR	COPIES ENCL
	PD1-1 LA		1	1	PD1-1 PD	1	1
	MENNING,J		2	2			
INTERNAL:	ACRS		6	6	NRR/DE/EELB	1	1
	NRR/DORS/OTSB		1	1	NRR/DRCH/HICB	1	1
	NRR/DSSA/SCSB		1	0	NRR/DSSA/SPLB	1	1
	NRR/DSSA/SRXB		1	1	NUDOCS-ABSTRACT	1	1
	OC/LFMB		1	0	OGC/HDS1	1	0
	REG FILE	01	1	1			
EXTERNAL:	NRC PDR		1	1	NSIC	1	1

NOTE TO ALL "RIDS" RECIPIENTS:

PLEASE HELP US TO REDUCE WASTE! CONTACT THE DOCUMENT CONTROL DESK, ROOM P1-37 (EXT. 504-2065) TO ELIMINATE YOUR NAME FROM DISTRIBUTION LISTS FOR DOCUMENTS YOU DON'T NEED!

TOTAL NUMBER OF COPIES REQUIRED: LTTR 22 ENCL 19

MAY

R I D S / A D D S

NIAGARA MOHAWK

NIAGARA MOHAWK POWER CORPORATION/301 PLAINFIELD ROAD, SYRACUSE, N.Y. 13212/TELEPHONE (315) 474-1511

May 14, 1993
NMP2L 1384

U. S. Nuclear Regulatory Commission
Attn: Document Control Desk
Washington, D.C. 20555

Re: Nine Mile Point Unit 2
Docket No. 50-410
NPF-69
TAC No. M86013

Gentlemen:

SUBJECT: FLAW IN HIGH PRESSURE CORE SPRAY NOZZLE SAFE END EXTENSION WELD - REQUEST FOR ADDITIONAL INFORMATION

On March 16, 1993 (NMP2L 1372), Niagara Mohawk Power Corporation (NMPC) submitted the results of its most recent fracture mechanics analysis on weld KC-32. In conjunction with NRC staff review of the submittal, a telephone conference was held on April 28, 1993 to address staff questions about the evaluation. At that time, it was agreed that a copy of a paper by Dedhia and Harris referred to in NMPC's submittal of June 28, 1991 (NMP2L 1306) entitled "Improved Influence Functions For Part-Circumferential Cracks In Pipes" would be provided. A copy of the paper is enclosed with this letter.

The staff also requested a copy of the point by point through-wall axial stress distribution for steady state operating temperatures. The table of data is also enclosed.

If you have any additional questions, please contact Mr. W. David Baker at 315-428-7029.

Very truly yours,

C. D. Terry
Vice President
Nuclear Engineering

200106

WDB/mls
003872GG
Enclosure
xc: Mr. T. T. Martin, Regional Administrator, Region I
Mr. R. A. Capra, Director, Project Directorate I-1, NRR
Mr. J. E. Menning, Project Manager, NRR
Mr. W. L. Schmidt, Senior Resident Inspector
Records Management

A001
1/1

Circumferential Cracks in Pressure Vessels & Piping - Vol II
PVP Vol 95, ASME, 1983

IMPROVED INFLUENCE FUNCTIONS FOR PART-CIRCUMFERENTIAL CRACKS IN PIPES[1]

D. D. Dedhia, Staff Engineer
Science Applications, Inc.
Palo Alto, California

D. O. Harris, Managing Engineer
Failure Analysis Associates
Palo Alto, California

ABSTRACT

Approximate influence functions for part-circumferential cracks in pipes or vessels are presented which are an improvement on previous results -- especially in the case of shallow cracks. The influence functions are useful in evaluating stress intensity factors for cracks of arbitrary depth and aspect ratio in bodies subjected to complex stress conditions. Details of the variation of K along the crack front are not obtainable from the influence functions; only "RMS-averaged" values are generated. Comparisons between local values of K and the RMS-averaged values are presented which show that the two sets of values are quite similar for most loading conditions of interest. Additionally, comparisons with results of other investigators in the limited cases where possible indicate that the improved functions provide accurate results for circumferential and axial cracks within the range of crack sizes analyzed. The applicability of the influence functions to longer cracks is discussed, and convenient curve fits suitable for numerical calculations are provided. A user-oriented computer code for evaluation of stress intensity factors that utilizes the improved influence functions is briefly described.

NOTATION

a	maximum crack depth
a_j	length of crack in "j" direction
A	crack area
b	half surface length of crack
g_1	a function in influence function formulation
g_2	a function in influence function formulation
h	pipe wall thickness

[1] Work supported by the Electric Power Research Institute, Palo Alto, California.

h_a influence function associated with depth direction ($\overline{K}_a$)

h_b influence function associated with length direction ($\overline{K}_b$)

h_j influence function associated with j-th direction ($\overline{K}_j$)

H equals $E/(1 - \nu^2)$, E -- Young's modulus, ν -- Poisson's ratio

$\overline{K}_a$ RMS-averaged stress intensity factor associated with depth direction

$\overline{K}_b$ RMS-averaged stress intensity factor associated with length direction

$\overline{K}_j$ RMS-averaged stress intensity factor associated with j-th direction

p exponent in power law stress (see Eq. 12)

r_i inside radius of pipe

R equals $[(x/a)^2 + (y/b)^2]^{1/2}$

U strain energy in cracked stressed body

w crack surface opening displacement

x spatial coordinate into pipe wall

y spatial coordinate in crack plane and normal to x

α equals a/h

β equals b/a

ΔA_a incremental change in crack area for a crack growing only in a direction

ΔA_b incremental change in crack area for a crack growing only in b direction

ΔA_j incremental change in crack area for a crack growing only in j-th direction

ξ equals $[1 - (x/a)^2 - (y/b)^2]$

θ equals $1 - \frac{2}{\pi} \tan^{-1} \frac{y/b}{x/a}$

σ normal stress on crack plane

σ_a normal stress at crack tip location prior to introduction of the crack

σ_B maximum value of stress in the case of through-thickness-bending

ϕ elliptical angle along crack front (equals 0 at point of maximum crack depth)

Φ complete elliptic integral of the second kind

INTRODUCTION

Stress intensity factors for semi-elliptical surface cracks in pipes or vessels are of interest in the analysis of subcritical and fast crack growth in these technologically important components. Stress intensity solutions for surface cracks in flat plates or longitudinal cracks in cylinders are available, and are too numerous to be covered here. However, with few exceptions, these solutions are available only for simple stress systems (uniform stress or Lamé solution for pressurized cylinders) and provide information only for a limited number of selected crack depths and lengths.

In order to overcome these deficiencies of earlier results, Reference 1 provided approximate influence functions [2,3] for part-circumferential cracks in cylinders. The curve fits provided in Reference 1 cover a wide range of arbitrary crack sizes and are applicable to the calculation of stress intensity factors for cracked cylinders with arbitrary stresses on the crack plane. Complex stress gradients, such as arise in thermal and residual stresses, can be accurately and economically treated by use of these influence functions. Additionally, the similarity between part-circumferential and longitudinal cracks in pipes is pointed out in References 1 and 4 for the range of crack sizes considered.

Comparisons of stress intensity factors generated by use of the influence functions in Reference 1 with previously existing solutions, showed that the influence function results were of sufficient accuracy for engineering purposes for cracks of intermediate depth. However, influence function results for shallow cracks were subject to greater inaccuracies, as is discussed in Reference 4. Recent concerns with pressure vessels subjected to severe thermal transients has led to increased interest in shallow cracks. The approximate influence functions of Reference 1 were therefore improved to provide greater accuracy for shallow cracks. The purpose of this paper is to present the improved influence functions and also to compare results generated by their use with additional K-solutions that have become available since Reference 1 was prepared.

Details of the variation of K along the crack front are not obtainable from the influence functions; only "RMS-averaged" values are generated. Comparisons between local values of K and corresponding RMS-averaged values are presented which show that the two sets of values are quite similar for most loading conditions of engineering importance. The RMS-averaged stress intensity factors for semi-elliptical cracks determined by use of influence functions are useful in the analysis of subcritical and fast crack growth. The major advantage of the influence functions over other techniques, such as finite elements, is the extreme economies realized when considering complex stresses in three-dimensional bodies [5]. A detailed discussion of the use of RMS-averaged stress intensity factors for crack growth analysis is beyond the scope of this paper. References 4 and 6-11 provide such discussions. Besuner [6] also includes consideration of the use of local values of K to analyze the fatigue growth of elliptical cracks. For the examples considered in Reference 6, the fatigue lifetimes calculated by use of local and RMS stress intensity factors agreed very closely. Additionally, Cruse [12] presents experimental results which indicates the suitability of RMS-averaged K values for analysis of fatigue crack growth.

The applicability of the influence functions provided here to longitudinal cracks in cylinders is discussed, and a user-oriented computer code [11] that utilizes the improved influence functions is briefly described.

IMPROVED INFLUENCE FUNCTIONS

The theory of influence functions for cracks in three-dimensional bodies has been covered elsewhere [2,3] and will be briefly reviewed. This will be followed by a presentation of the improved influence functions and a discussion of numerical procedures for using them to calculate stress intensity factors. Comparisons with results from other investigations and additional discussions will be included in later sections.

Review of Influence Functions

The part-circumferential crack shown in Figure 1 will be considered for the case of symmetry with respect to the line AB. Such a crack is considered to have "two degrees-of-freedom" associated with growth in the depth (a) and length (b) directions. Denoting these as the 1 and 2 directions respectively, the following expressions for the RMS-averaged stress intensity factors (K_a, K_b or K_j, j = 1, 2) apply

$$K_j = \int_A h_j(x,y,a,b)\ \sigma(x,y)dA$$

$$= \left\{ \frac{1}{\Delta A_j} \int_0^{\pi/2} K^2(\phi)\ d[\Delta A_j(\phi)] \right\}^{1/2} \qquad (1)$$

The first integral is performed over the area of the crack using the stresses on the crack plane prior to introduction of the crack. The parameters $\Delta A_j(\phi)$ are associated with incremental crack area changes for cracks growing only in the j-th direction [2-4,11]. The RMS-averaged stress intensity factors are closely related to the strain energy release rates for semi-elliptical cracks growing in each of the directions corresponding to the degrees-of-freedom. The cracks remain semi-elliptic as they extend, but the crack aspect ratio can change. The close relationship between $\bar{K}_j$ and the strain energy release rates is a basis of their suitability for analysis of subcritical and fast crack growth.

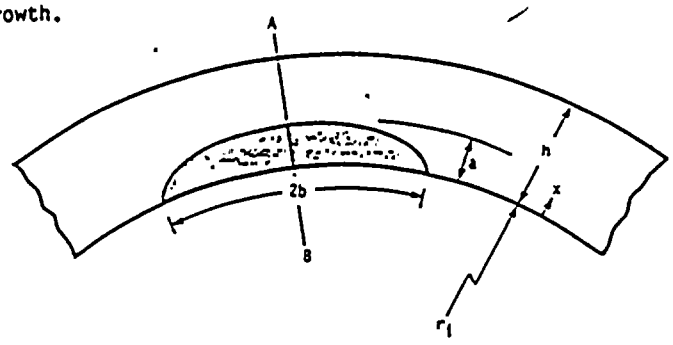

$\beta = \frac{b}{a}$

$\alpha = \frac{a}{h}$

Figure 1. Geometry of Part-Circumferential Internal Surface Crack Considered in This Investigation.

Following the development of Cruse and Besuner [3,6-8], the influence function h_j is given by

$$h_j = \frac{\partial w}{\partial a_j} \Big/ \left[\frac{1}{H}\frac{\partial A}{\partial a_j}\frac{\partial U}{\partial a_j}\right]^{1/2} \tag{2}$$

where $a_1 = a$ and $a_2 = b$. h_j can be evaluated from numerical solutions for crack surface displacements for a reference stress system. In order to minimize errors in development of the influence functions, the known influence function for an embedded elliptical crack in an infinite body is utilized with corrections made to account for the free surfaces of the cylinder. Following earlier developments [1,4,7,8,11], the influence function, h_j, for a part-circumferential crack is expressed in terms of the known influence function (h_j^*) strain energy (U^*) and crack surface displacement (w^*) for the embedded elliptical crack by the following:

$$h_j = h_j^* \left[g_2 + w^* \frac{\partial g_2}{\partial a_j} \Big/ \frac{\partial w^*}{\partial a_j}\right] \Big/ \left[g_1 + U^* \frac{\partial g_1}{\partial a_j} \Big/ \frac{\partial U^*}{\partial a_j}\right]^{1/2} \tag{3}$$

The functions g_1 and g_2 are numerically evaluated as ratios of the strain energy and crack surface displacements, respectively, for the surface crack to the embedded crack. Hence, the desired approximate influence functions are known once the functions g_1 and g_2 are evaluated. For the sake of completeness, the following closed-form results for the embedded crack are included [7,8]

$$w^* = \frac{2\sigma a}{H\Phi}\xi^{1/2} \tag{4}$$

$$U^* = \frac{4\pi\sigma^2 a^2 b}{3 H \Phi} \tag{5}$$

uniform stress

$$h_a^* = \frac{\left[\frac{1}{a} - \frac{1}{\phi}\frac{\partial\phi}{\partial a} + \frac{x^2}{a^3\xi}\right]\xi^{1/2}}{\pi\, b\left[\frac{1}{3}\phi\left(\frac{2}{a} - \frac{1}{\phi}\frac{\partial\phi}{\partial a}\right)\right]^{1/2}} \tag{6}$$

$$h_b^* = \frac{\left[\frac{1}{\phi}\frac{\partial\phi}{\partial b} + \frac{y^2}{b^3\xi}\right]\xi^{1/2}}{\pi\left[\frac{ab}{3}\phi\left(\frac{1}{b} - \frac{1}{\phi}\frac{\partial\phi}{\partial b}\right)\right]^{1/2}} \tag{7}$$

ϕ is the complete elliptic integral of the second kind, which is defined as follows.

$$\phi(a/b) \equiv \int_0^{\pi/2}\left[1 - \left(1 - \frac{a^2}{b^2}\right)\sin^2\psi\right]^{1/2} d\psi \tag{8}$$

A convenient approximation of ϕ is

$$\phi(a/b) \sim \left[1 + 1.464\left(\frac{a}{b}\right)^{1.65}\right]^{1/2} \tag{9}$$

This approximation is good for $a < b$, and is accurate to within 0.13% for a/b between 0 and 1.

Improved Influence Functions

The functions g_1 and g_2 were evaluated earlier [1,4]. Cracks with α = 0.25, 0.4, 0.5, 0.6, 0.8 and β = 1-6 were analyzed using the boundary integral equation (BIE) technique, thereby producing numerous data points for g_1 and g_2. These data were then used to curve fit functions for g_1 and g_2. The functional forms assumed by Besuner [6] for a semi-elliptical surface crack in a half-space (α = 0) were utilized. However, the earlier curve fits were optimized for intermediate crack depths and do not reduce to Besuner's results for w In order to improve the influence function for shallow cracks (small α), slightly modified forms for g_1 and g_2 were utilized, and the numerical data generated earlier were then used to evaluate constants in the assumed functional form.

The curve fit for g_1 is fairly straightforward because this function depends on only two variables, α and β (for a given r_i/h). The improved function g_1 was obtained by using the numerical values of g_1 for the cracks analyzed earlier in combination with corresponding values from Besuner [7] for α = 0. The coefficients in the assumed functional form were determined by least squares. The following result was obtained

$$g_1 = (1.1328 + 0.05753\beta - 0.007625\beta^2) + (-0.12727 + 0.4902\beta - 0.06515\beta^2)\alpha + (-0.3005 + 0.73192\beta - 0.2839\beta^2 + 0.03572\beta^3)\alpha^2 \tag{10}$$

The fit for g_2 is more involved, because g_2 is a function of four variables; x, y, a, b. Besuner [7] assumes a functional form for g_2 for α = 0. In the present case, this same functional form is assumed, and g_2 is now required to reduce exactly to Besuner's results as α approaches zero. (This is in contrast to the earlier approach [1,4] which did not impose the condition that g_2 reduce exactly to Besuner's result for α = 0). The previously generated numerical values for g_2 were then used to evaluate some additional constants to account for α not being zero. The following results were obtained

$$g_2 = A_0(\alpha) + A_1 R^{1.5}\theta^{0.15} + A_2 R^{1.5}\theta^{0.3} + A_3 R^{2.5}\theta^{0.15} + A_4(\alpha) R^{2.5}\theta^{0.3} + A_5(\alpha)\left(\frac{a}{b} - 1\right) + A_6(\alpha)\left(\frac{a}{b} - 1\right)^2 \quad (11)$$

where

$$R = \left[\left(\frac{x}{a}\right)^2 + \left(\frac{y}{b}\right)^2\right]^{1/2}$$

$$\theta = 1 - \frac{2}{\pi}\left\{\tan^{-1}\frac{y/b}{x/a}\right\}$$

$$A_0(\alpha) = 1.323 + 0.13831\alpha + 0.60229\alpha^2$$

$$A_1 = 0.54443$$

$$A_2 = -1.27014$$

$$A_3 = -0.55144$$

$$A_4(\alpha) = 0.98756 - \alpha$$

$$A_5(\alpha) = -0.06579 - 0.52508\alpha + 0.43354\alpha^2$$

$$A_6(\alpha) = 0.01471 - 0.82792\alpha + 2.6834\alpha^2$$

This reduces exactly to Besuner's g_2 for $\alpha = 0$. Obviously, the α dependence is accounted for entirely in the A_0, A_4, A_5 and A_6 terms.

Numerical Evaluations

The influence functions, h_i, are known once g_1 and g_2 are available (see Eq. 3). Stress intensity factors, K_i, can then be evaluated by numerical integration (see Eq. 1). In practice, such calculations are fairly intricate and further complicated by the presence of a singularity in the influence function. Procedures for economically and accurately performing the numerical integration are briefly discussed in Reference 4 (page 302). In order to make the influence functions more usable and generally available, a user-oriented code was written which will automatically provide stress intensity factors once the stresses and crack sizes are defined. Reference 11 describes the code and its use. The code can also treat complete circumferential cracks and plane strain axial cracks by use of the corresponding weight functions provided by Labbens, et al. [13]. Results generated by the use of this code will be presented in the following section, where comparison with the results of other investigations will be provided.

COMPARISONS AND DISCUSSION

Stress intensity factors generated by use of the improved influence functions will be compared with recent results of other investigations in order to assess the accuracy of the influence functions. Corresponding local and RMS-values of K will be included, and a discussion of the applicability of the influence functions to axial cracks and cracks with β greater than 6 will be provided.

Comparisons

Numerous comparisons of stress intensity factors generated by use of the older influence functions with results of other investigators are provided in References 1 and 4. In general, it was found that the agreement was quite good

for the limited range of crack sizes for which other solutions were available. Additionally, for the range of crack sizes in which comparisons were possible, ($\alpha < 0.8$, $\beta = 1$-6) it was found that part-circumferential and axial cracks were very similar and the value of r_i/h had only a small influence on K. Recent results by Raju and Newman [14] provide information for crack sizes and stress gradients beyond previously available information. Their results provide local values of K along the crack front [$K(\phi)$], which were converted to RMS-averaged values ($\overline{K}_i$) by numerical integration of the second form of Eq. (1). Raju and Newman provide results for discrete selected crack sizes corresponding to $\alpha = 0.2, 0.5, 0.8$, $\beta = 1, 2.5, 5$, and stresses on the crack plane varying as

$$\sigma(x) = (x/a)^p \qquad (12)$$

with $p = 0, 1, 2, 3$. Their results are for longitudinal cracks in cylinders with $r_i/h = 10$.

Figures 2-4 provide comparisons of the results of Raju and Newman [14] with corresponding values generated by the improved influence functions. The results are expressed in terms of σ_a - the stress at the location of maximum crack depth prior to introduction of the crack.

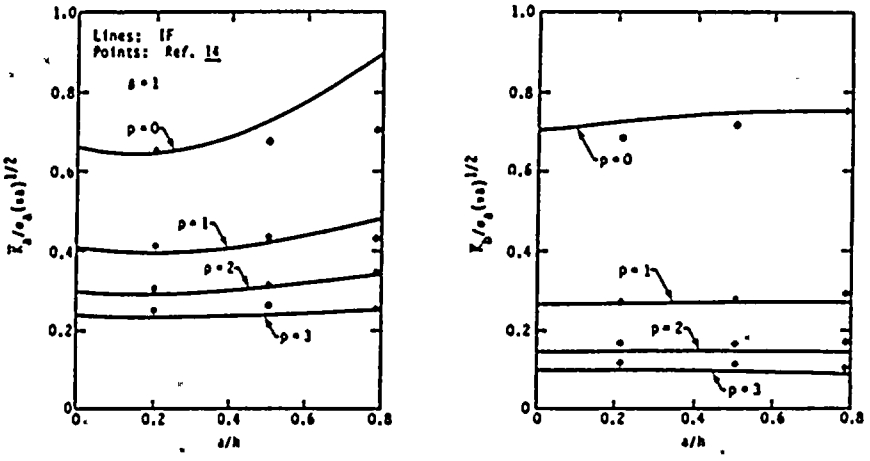

Figure 2. Comparison of Influence Function Results for Power Stresses with Results of Raju and Newman [14]. IF Results are for Circumferential Crack with $r_i/h = 5$; Ref. 14 Results are for Axial Crack with $r_i/h = 10$.

In general, very good agreement is observed, with errors typically below 5%. The poorest agreement is for deep cracks, especially for small β, where errors as large as 25% are present. The agreement improves for shallower cracks, as expected based on earlier discussions, and the results reduce exactly to Besuner's values as α goes to zero. Comparisons with results of other investigators, such as Heliot, et al. [15] were also made with equally good agreement being obtained. Thus, it is felt that the improved influence functions provide accurate results for $\overline{K}_i$ for a wide range of crack sizes under an arbitrary system of stresses. The use of these results for $\beta > 6$ and/or $\alpha > 0.8$ is open to question and will be discussed shortly.

Local and RMS-Values

The inability of the influence functions to provide information on the variation of K along the crack front is one drawback of this approach. However, practical applications of stress intensity factors involve their use in some

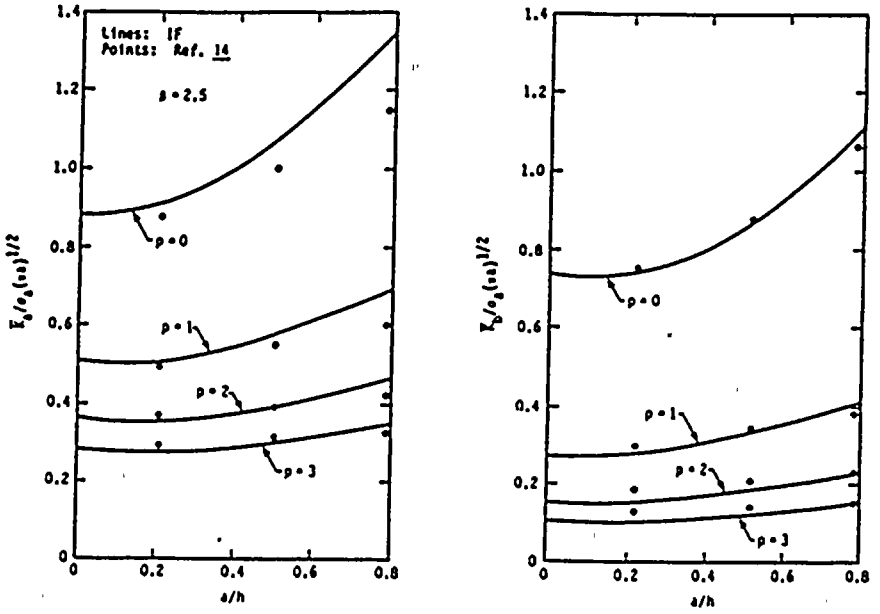

Figure 3. Comparison of Influence Function Results for Power Stresses with Results of Raju and Newman [14]. IF Results are for Circumferential Crack with $r_i/h = 5$; Ref. 14 Results are for Axial Crack with $r_i/h = 10$.

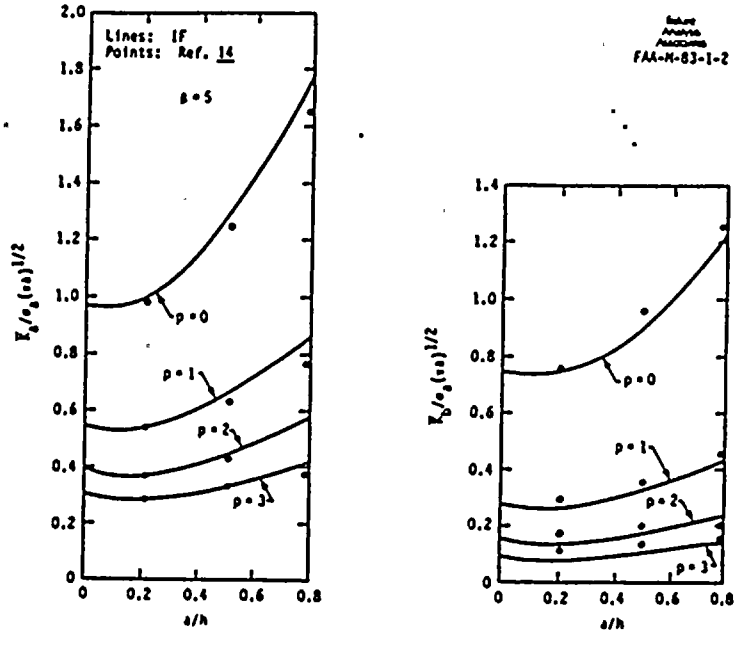

Figure 4. Comparison of Influence Functions for Power Stresses with Results of Raju and Newman [14]. IF Results are for Circumferential Crack with $r_i/h = 5$; Ref. 14 Results are for Axial Crack with $r_i/h = 10$.

form of crack growth law or fracture criterion. The question then arises as to whether local values of K are required, or are RMS-averaged values (strain energy release rates) adequate. Both local and RMS-averaged values have been used in fracture mechanics analyses. Table 1 presents some direct comparisons between local and RMS stress intensity factors. It is seen that, in general, the two sets of values are not radically different. The percentage differences are large only if the absolute values of K are small. Additionally, consideration of rather artificial stress gradients [such as $(x/a)^3$] is somewhat confusing. Therefore, results for a linear stress gradient ("through-thickness-bending"), in which

$$\sigma(x/h) = \sigma_B(1 - 2x/h) \qquad (13)$$

are also included in Table 1. Comparisons of the technologically important cases of uniform stress ($p = 0$) and through-thickness-bending reveals that the two sets of values are within 12% of each other for $p = 0$ and usually within 25% for through-thickness-bending. Thus, it appears that the RMS-values would usually be of sufficient accuracy for most engineering purposes -- even if a local K approach was considered to be more suitable.

Additional Discussion of Applicability of Results

As briefly mentioned in the introduction of this paper, and discussed more fully in References 1 and 4, comparisons of stress intensity factors for circumferential and axial cracks (in the limited number of cases where such comparisons are possible) indicate that the crack orientation has a negligible influence on K and that r_i/h has only a small influence. Such comparisons are possible only for β in the range of 1-6 and $\alpha < 0.8$. The question then arises as to whether the different crack orientations would also behave similarly for larger aspect ratios, and would the value of r_i/h still have a fairly small influence?

Comparison of K-values for uniform stress are not particularly revealing. Such comparisons for through-thickness bending are somewhat more informative, and Figure 5 presents such results for three cases: (i) complete circumferential crack (very large β), (ii) part-circumferential crack with $r_i/h = 5$, and (iii) axial crack with $r_i/h = 10$. From these figures, it would be tempting to again conclude that r_i/h has a small influence, and crack orientation is not important. Furthermore, the results for $\beta = 5$ are already close to the values for a complete circumferential crack (very large β), so that it appears that K will not increase appreciably as β increased beyond 5 -- even for axial cracks.

However, additional insights can be gained by considering various two-dimensional problems with through-thickness-bending. Various stress intensity factor results are presented in Figure 6. The flat plate values correspond to an infinite value of r_i/h and are for a strip in pure bending [16]. The axial and circumferential crack results were generated by use of the computer code described in Reference 11, which, in this particular instance, utilizes Labbens, et al. [13] influence functions. Results obtained by use of the closed form influence function for a periodic array of equally spaced co-planar cracks in an infinite sheet [Reference 16, page 7.7] are also shown. This latter geometry can serve as a relatively simple model of a body whose deformation is constrained in a manner somewhat similar to pipes. This is discussed more fully in References 10 and 17, in which it is shown that if the stresses are self-equilibrating through the thickness, then K approaches zero as the crack depth approaches the value of the thickness. That is

$$\lim_{a \to h} K = 0 \text{ if } \int_0^h \sigma(x)dx = 0$$

This behavior is observed in Figure 6 for the axial and circumferential cracks in pipes with finite r_i/h but not for the flat plate (infinite r_i/h). This

INFLUENCE FUNCTIONS BASED ON LOCAL VALUES FROM THIS TABLE.

Table 1
Comparison of Local and RMS-K Values

			β = 1		β = 2.5		β = 5	
p*	α	RMS, local†	a‡	b§	a	b	a	b
0	0.2	R	0.653	0.681	0.877	0.738	0.982	0.617
		L	0.646	0.726	0.932	0.676	1.062	0.578
	0.5	R	0.678	0.718	0.990	0.861	1.248	0.954
		L	0.669	0.777	1.058	0.814	1.359	0.753
	0.8	R	0.702	0.764	1.155	1.046	1.656	1.255
		L	0.694	0.858	1.211	1.060	1.783	1.123
1	0.2	R	0.403	0.264	0.494	0.283	0.535	0.287
		L	0.455	0.125	0.584	0.109	0.641	0.075
	0.5	R	0.412	0.274	0.536	0.320	0.627	0.350
		L	0.464	0.141	0.629	0.153	0.746	0.132
	0.8	R	0.425	0.284	0.597	0.372	0.786	0.451
		L	0.484	0.162	0.701	0.225	0.914	0.241
2	0.2	R	0.305	0.154	0.358	0.163	0.381	0.165
		L	0.375	0.047	0.455	0.037	0.490	0.022
	0.5	R	0.309	0.158	0.378	0.179	0.426	0.194
		L	0.380	0.054	0.477	0.060	0.544	0.050
	0.8	R	0.318	0.161	0.412	0.202	~~0.310~~ 0.358	0.198
		L	0.394	0.063	0.523	0.092	0.639	0.099
3	0.2	R	0.249	0.105	0.284	0.110	0.288	0.108
		L	0.326	0.024	0.383	0.018	0.417	0.010
	0.5	R	0.251	0.107	0.297	0.119	0.327	0.128
		L	0.328	0.028	0.397	0.031	0.440	0.026
	0.8	R	0.258	0.109	0.319	0.131	0.374	0.152
		L	0.339	0.032	0.429	0.049	0.504	0.053
‖	0.2	R	0.819	1.043	1.132	1.045	1.279	1.065
		L	0.773	1.126	1.164	1.054	1.311	0.914
	0.8	R	-0.036	-0.514	-0.333	-0.753	-0.711	-0.888
		L	0.134	-0.998	-0.149	-1.166	-0.535	-1.032

Source: Results provided by Raju and Newman [14].
Note: Values shown are $K_I/\sigma_a(\pi a)^{1/2}$.

* p in Eq. (12)
† R - RMS averaged value, L - local value
‡ a - depth direction
§ b - surface length direction
‖ Through-thickness bending, see text. Results for α = 1/2 omitted because $\sigma_a = 0$.

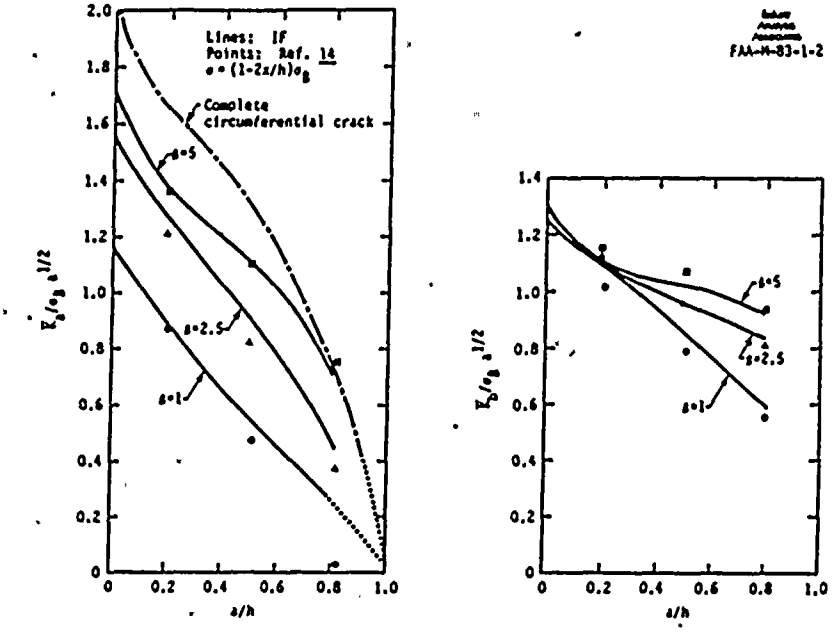

Figure 5. Comparison of IF Solutions for Through-Thickness Bending Stress With Corresponding Results [14]. IF Results are for Circumferential Crack with $r_i/h = 5$; Ref. 14 Results are for Axial Crack with $r_i/h = 10$.

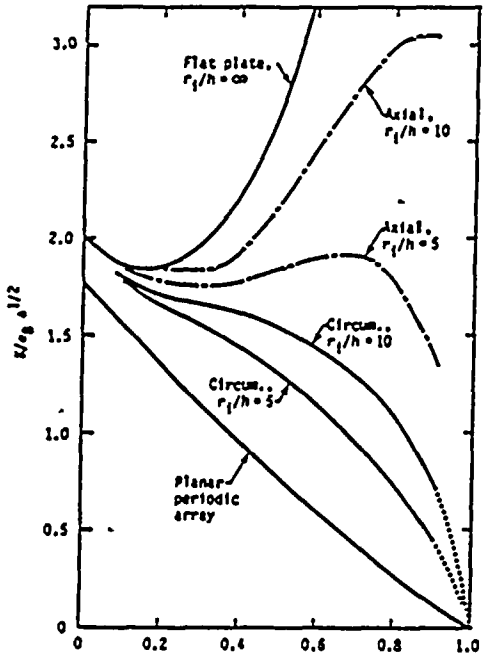

Figure 6. K for Through-Thickness Bending in Pipes With One-Dimensional Cracks of Axial or Circumferential Orientation.

marked difference in behavior of flat plates and pipes is not surprising, because of the markedly different ways that they can support loads.

Figure 6 shows that marked differences are not observed for shallow cracks, but that axial and circumferential cracks can have marked differences for deeper cracks. Furthermore, the value of r_i/h can be important (even in the range of 5-10) for very long deep cracks -- especially when through-wall stress gradients are present. Therefore, it appears that the present influence functions for semi-elliptical cracks provide results of reasonable accuracy for most engineering purposes for both axial and circumferential cracks for $\beta < \sim 6$. Results for $\beta > 6$ are also most likely quite accurate for circumferential cracks, but application of the influence functions to long deep axial cracks could produce unconservative errors, especially in the case of large r_i/h and in the presence of stress gradients. Therefore, the use of the improved influence functions for long deep axial cracks could be unconservative, and more accurate stress intensity factors for this configuration await future development.

SUMMARY AND CONCLUSIONS

Approximate influence functions for part-circumferential cracks in pipes are presented that are more accurate than previously published results -- especially in the case of shallow cracks. The influence functions are applicable to a wide variety of sizes of cracks subjected to arbitrary stresses. In the limited number of cases where this is possible, comparisons of results generated by the improved influence functions to corresponding results of other investigators indicate that the influence functions are capable of providing accurate results. A computer code that uses the influence functions to provide stress intensity factors by numerical integration is briefly described. Local values of K along the crack front are not provided by use of the influence functions; only RMS-averaged values are obtainable. Comparison between local (surface and maximum crack depth) values and corresponding RMS-values are provided which show that these two sets of values are not widely different, especially in the technologically important cases of uniform stress and linear stress gradient.

Additional discussion of the applicability of the influence function results indicates that they are capable of providing accurate results for both axial and circumferential cracks in the range of crack sizes considered ($a/h < 0.8$, $b/a < 6$), and for r_i/h in the range of 5-10. Furthermore, it appears that the influence functions provide reasonable results for circumferential cracks for $\beta > 6$. However, application of the influence functions to deep axial cracks with $\beta > 6$ may be unconservative.

ACKNOWLEDGEMENTS

The support provided for this work by the Electric Power Research Institute in Palo Alto, California is gratefully acknowledged. The informative and stimulating discussions with Dr. D.M. Norris and Mr. T.J. Griesbach (of the Nuclear Safety Analysis Center) were especially helpful.

REFERENCES

1. Lim, E. Y., Dedhia, D. D., and Harris, D. O., "Approximate Influence Functions for Part-Circumferential Interior Surface Cracks in Pipes," to appear in Fracture Mechanics: Fourteenth Symposium, ASTM Special Technical Publication 791, Philadelphia, Pennsylvania, 1983.

2. Rice, J. R., "Some Remarks on Elastic Crack Tip Stress Fields," International Journal of Solids and Structures, Vol. 8, pages 751-758, 1972.

3. Cruse, T. A., and Besuner, P. M., "Residual Life Prediction for Surface Cracks in Complex Structural Details," Journal of Aircraft, Vol. 12, No. 4, pages 369-375, April 1975.

4. Harris, D. O., Lim, E. Y., and Dedhia, D. D., "Probability of Pipe Fracture in the Primary Coolant Loop of a PWR Plant, Vol. 5: Probabilistic Fracture Mechanics Analysis," U.S. Nuclear Regulatory Commission Report NUREG/CR-2189, Vol. 5, Washington, D.C., 1981.

5. Besuner, P. M., and Caughey, W. R., "Comparison of Finite Element and Influence Function Methods for Three-Dimensional Elastic Analysis of Boiling Water Reactor Feedwater Nozzle Cracks," Electric Power Research Institute Report NP-261, Palo Alto, California, 1976.

6. Besuner, P. M., "Residual Life Estimates for Structures with Partial Thickness Cracks," Mechanics of Crack Growth, ASTM Special Technical Publication 590, Philadelphia, Pennsylvania, pages 403-419, 1976.

7. Besuner, P. M., et al., "BIGIF: Fracture Mechanics Code for Structures," Electric Power Research Institute Report EPRI NP-838, Palo Alto, California, 1978.

8. Besuner, P. M., "The Influence Function Method for Fracture Mechanics and Residual Life Analysis of Cracked Components Under Complex Stress Fields," Nuclear Engineering and Design, Vol. 43, No. 1, 1977, pages 115-154.

9. Dedhia, D. D., Harris, D. O., and Lim, E. Y., "The Influence of Non-Uniform Thermal Stresses on Fatigue Crack Growth of Part-Through Cracks in Reactor Piping," to appear in Fracture Mechanics: Fourteenth Symposium, ASTM Special Technical Publication 791, Philadelphia, Pennsylvania, 1983.

10. Harris, D. O., and Dedhia, D. D., "The Influence of Residual Stresses on the Growth of Semi-Elliptical Stress Corrosion Cracks in Pipes," submitted for presentation at ASME Pressure Vessel and Piping Conference, Portland, Oregon, June 1983.

11. Dedhia, D. D., and Harris, D. O., "Stress Intensity Factors for Surface Cracks in Pipes: A Computer Code for Evaluation by Use of Influence Functions," Electric Power Research Institute Report EPRI NP-2425, Palo Alto, California, June 1982.

12. Cruse, T. A., Myers, G. J., and Wilson, R. B., "Fatigue Growth of Surface Cracks," Flaw Growth and Fracture, ASTM Special Technical Publication 631, Philadelphia, Pennsylvania, pages 174-189, 1977.

13. Labbens, R., Pellisier-Tanon, A., and Heliot, J., "Practical Method for Calculating Stress Intensity Factors Through Weight Functions," Mechanics of Crack Growth, ASTM Special Technical Publication 590, Philadelphia, Pennsylvania, pages 368-384, 1976.

14. Raju, I. S., and Newman, J. C., Jr., "Stress Intensity Influence Coefficients for Internal and External Surface Cracks in Cylindrical Vessels," Aspects of Fracture Mechanics in Pressure Vessels and Piping PVP Vol. 58, American Society of Mechanical Engineers, New York, New York, pages 37-48, 1978.

15. Heliot, J., Labbens, R. C., and Pellisier-Tanon, A., "Semi-Elliptical Cracks in a Cylinder Subjected to Stress Gradients," Fracture Mechanics, ASTM Special Technical Publication 677, Philadelphia, Pennsylvania, pages 341-364, 1979.

16. Tada, H., Paris, P. C., and Irwin, G. R., Stress Analysis of Cracks Handbook, Del Research Corporation, Hellertown, Pennsylvania, 1973.

17. Harris, D. O., Lim, E. Y., Dedhia, D. D., Woo, H. H., and Chou, C. K., "Fracture Mechanics Models Developed for Piping Reliability Assessment in Light Water Reactors," U.S. Nuclear Regulatory Commission Report NUREG/CR-2301, Washington, D.C., 1982.

Through-wall Axial Stress Distribution due to Steady-State Operating Temperature (552°F)

	Wall Fraction	Axial Stress (ksi)
1	0.	7.028
2	0.2083E-01	6.083
3	0.4167E-01	5.139
4	0.6250E-01	4.194
5	0.8333E-01	3.250
6	0.1042	2.305
7	0.1250	1.361
8	0.1458	0.8277
9	0.1667	0.2946
10	0.1875	-.2385
11	0.2083	-.7715
12	0.2292	-1.305
13	0.2500	-1.838
14	0.2708	-2.225
15	0.2917	-2.613
16	0.3125	-3.000
17	0.3333	-3.388
18	0.3542	-3.775
19	0.3750	-4.163
20	0.3958	-3.971
21	0.4167	-3.778
22	0.4375	-3.586
23	0.4583	-3.393
24	0.4792	-3.201
25	0.5000	-3.008
26	0.5208	-2.860
27	0.5417	-2.713
28	0.5625	-2.565
29	0.5833	-2.417
30	0.6042	-2.269
31	0.6250	-2.122
32	0.6458	-1.760
33	0.6667	-1.399
34	0.6875	-1.037
35	0.7083	-.6754
36	0.7292	-.3138
37	0.7500	0.4778E-01
38	0.7708	0.5076
39	0.7917	0.9675
40	0.8125	1.427
41	0.8333	1.887
42	0.8542	2.347
43	0.8750	2.807
44	0.8958	3.408
45	0.9167	4.009
46	0.9375	4.611
47	0.9583	5.212
48	0.9792	5.813
49	1.000	6.415

Extracted from: "Parametric Crack Growth Study on the 10" Core Spray Nozzle (N16) Safe-end to Extension Weld KC-32", O'Donnell Safety-related workbook by E. Danfelt, verified by B. Kasraie, Project #2174, May-June 1991.